Quantitative characterization of micromixing simulation

Zhiyi Zhang,[1,a)] ChaeHo Yim,[2] Min Lin,[3] and Xudong Cao[2,a)]
[1]*Institute for Microstructural Science, National Research Council Canada, Ottawa, Ontario K1A 0R6, Canada*
[2]*Department of Chemical Engineering, University of Ottawa, Ottawa, Ontario K1N 6N5 Canada*
[3]*Canadian Food Inspection Agency, Ottawa, Ontario K2H 8P9, Canada*

(Received 30 April 2008; accepted 11 July 2008; published online 11 August 2008)

Micromixers with floor-grooved microfluidic channels have been successfully demonstrated in experiment. In this work, we numerically simulated the mixing within the devices and used the obtained concentration versus channel length profiles to quantitatively characterize the process. It was found that the concentration at any given cross-section location of the microfluidic channel periodically oscillates along the channel length, in coordination with the groove-caused helical flow during the mixing, and eventually converges to the neutral concentration value of two the mixing fluids. With these data, the specific channel length required for each helical flow to complete, the mixing efficiency of the devices, and the total channel length required to complete a mixing were easily defined and quantified, and were used to directly and comprehensively characterize the micromixing. This concentration versus channel length profile-based characterization method was also demonstrated in quantitatively analyzing the micromixing within a classic *T* mixer. It has clear advantages over the traditional concentration image-based characterization method that is only able to provide qualitative or semiquantitative information about a micromixing, and is expected to find an increasing use in studying mixing and optimizing device structure through numerical simulations. © *2008 American Institute of Physics.* [DOI: 10.1063/1.2966454]

I. INTRODUCTION

Micromixing is one of the most common and important functions of microfluidic devices. However, this process is extremely slow since it is purely dictated by passive molecular diffusions due to the laminar nature of the fluid flow within the microfluidic channels, as a result of the small dimensions of the channels and slow flow rates of the fluids within the channels.[1] Therefore many mixing technologies, both active and passive in nature, have been developed to overcome this problem in an attempt to achieve complete mixings within a reasonable time and microchannel length scale. Among all of the successfully studied microchannel designs, micromixers with grooved surfaces (i.e., floor-grooved micromixers) have brought up intensive interests and have been used in some applications. The grooved micromixers use a series of patterned grooves on the inner channel surface to stretch and fold volumes of fluids to be mixed over the cross section of the channel to reduce the distance that different molecules have to diffuse to mix.[2,3] These designs have been shown to be more efficient than most of their passive micromixer counterparts, and they are simpler, inexpensive to fabricate, and more practical than active micromixers that generally use external energy, in additional to the pumping energy, to stir the fluids to achieve efficient mixing and require complicated device packaging and system integration.

While significant amount of work has been devoted to experimentally demonstrating the

[a)]Authors to whom correspondence should be addressed. Electronic mail: zhiyi.zhang@nrc-cnrc.gc.ca and xcao@eng.uottawa.ca.

efficacy of the grooved micromixers in mixing, computational studies based on computational fluid dynamics (CFD) simulation have also been carried out to characterize and more importantly to understand the mixing process in the micromixers. To this end, computer simulations have been used to visualize both single and double helical flows caused by the slanted grooves and staggered herringbone grooves within the microchannels, respectively, under both pressure-drive[4–12] and electro-osmotic flows.[13] It has been shown that the simulation results are in good agreement with the experimental results of the micromixers.[2,3,7–9] It has also been concluded from the simulations that helical flows are affected by the groove geometries, such as the groove depth, width, and inclination,[8,10,11] and that the helical flows can occur even when the Reynolds number is low and the Peclet number is high.[9,12,14] While there is progress in simulating the micromixing and numerical simulation has become an easy task with available commercial software, it is still impractical to truly design a micromixer in a way that the optimal device structure for a specific application can be easily found through numerical simulations so that experimental trials can be minimized, as demonstrated in the design and fabrication of microelectronic and integrated photonic devices. The reason is that the current characterization methods, such as image analysis, are unable to find effective ways to quantitatively, directly, and comprehensively characterize the simulation results even though the numerical simulation of micromixing, by itself, is a quantitative method and each simulation can generate a lot of important information about the process. In the process of designing a high-efficient grooved micromixer for our targeted microfluidic-based flow cytometer with small channel dimension, we were forced to find a meaningful way to characterize our simulation results and thus optimize the device structure. We have found that the concentration versus channel length profiles of the mixing fluids can provide quantitative data to directly characterize the whole mixing process and device performance as reported in this paper, which makes a true device design possible.

II. NUMERICAL SIMULATION

This work was focused on the evaluation of molecular mixing of two different fluids within the microfluidic channels with grooved surface. The numerical simulation was to solve incompressible Navier-Stokes equations and convection-diffusion equations at steady state[8] using the CFD functions of COMSOL Multiphysics (version 3.1), assuming that the mixing within a grooved micromixer is dictated by both bulk advections caused by the grooves and molecular diffusions between the fluids. A miniaturized version of the reported slant-grooved micromixer (SGM)[3,4] was used in the simulation with some modifications as shown in Fig. 1. The micromixer had a rectangular microfluidic channel with a cross-section dimension of 20 μm (height) $\times 50$ μm (width) in its mixing section. On its channel floor surface of the mixing section, slanted grooves of 5 μm deep and 12.5 μm wide were patterned at a 45° angle to the flow direction along channel length. The two inlet channels of the micromixer that introduce two mixing fluids were abridged to focus on the mixing section only, and the inlet flows were set as laminar flows. The boundary conditions were set as follows: Outflow gauge pressure of the channel as 0 Pa ($p=0$), velocity of the flows at the channel walls as 0 m/s ($u=0$), and inlet concentrations as 1 M for one fluid initially occupying half of the channel cross section and 0 M for another fluid initially occupying the other half of the channel cross section. Here, both the fluids were composed of the same type of solute and solvent. Other parameters used in the simulation included 0.01 m/s for the average linear velocity of both fluids at the inlet, and 10^{-10} m^2/s for the molecular diffusion coefficient for the solute in the solvent. The corresponding Reynolds number $\mathrm{Re}=l\rho\nu/\eta$ of the studied fluids was estimated to be 0.03 when the fluids are aqueous solutions with density $\rho=1$ g/cm^3 and viscosity $\eta=0.001$ Ns/m^2.

A tetrahedral free meshing method, with maximum element size scaling factor at 0.2, element growth rate at 1.3, mesh curvature factor at 0.2, mesh curvature cutoff at 0.001 and resolution of narrow region at 1, was used in the simulation. It combined a triangular grid system with the tetrahedral grid at the wall region to capture the gradient near walls. There were 1.0×10^6 to 1.5×10^6 of tetrahedral elements and 1.4×10^5 to 1.8×10^5 of triangular elements involved in the

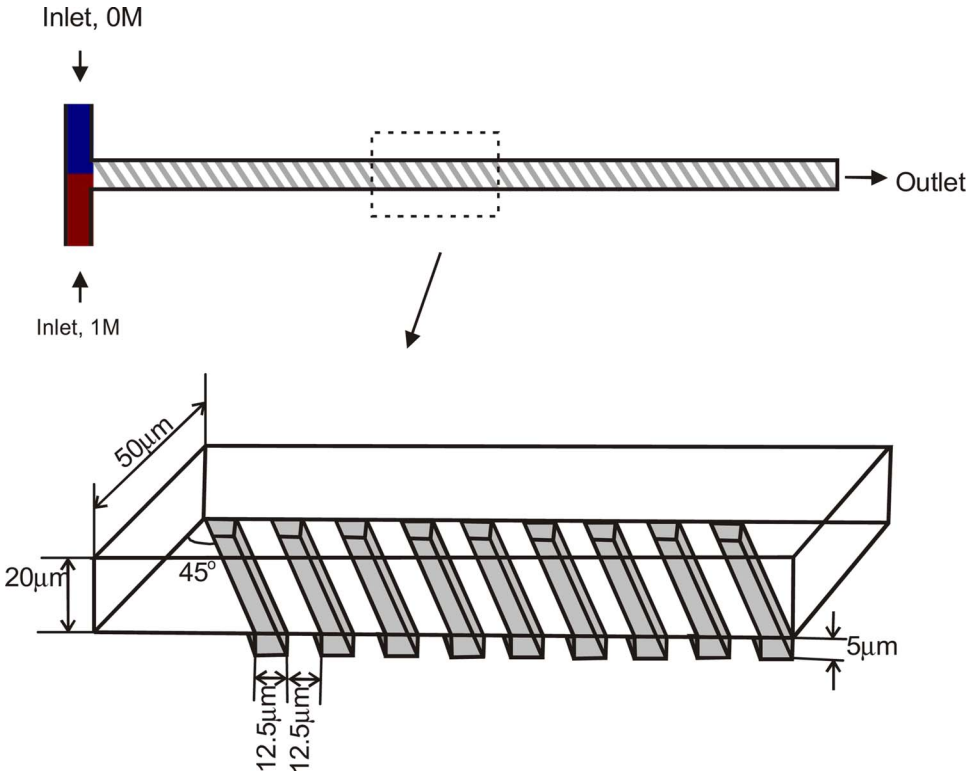

FIG. 1. The geometry of the slant-grooved micromixer (SGM) where the groove depth can be changed from the indicated 5 μm to 10, 20, or 30 μm.

simulation, in which mesh was adjusted according to each specific device structure and mixing condition to achieve the required convergence at a reasonable time scale while maintaining the required accuracy.

III. RESULTS AND DISCUSSION

The micromixer used in this study was a 75% proportionally reduced version of the SGM reported in the literature,[7] as such the channel dimension is compatible with our targeted microfluidic flow cytometer that integrates cell labeling and optical detection on one chip. Figure 2 shows the simulation results of the micromixer. The cross-section streamlines [Fig. 2(a)] and the upper-surface concentration image [Fig. 2(b)] of the mixing fluids within the channel show a typical helical flow, where some of the fluids near channel floor fall into the grooves and cause the helical flow within the channel with strong bulk advections near the channel floor and with a rotation of the involved two fluids within the channel. The results are similar to the reported simulation and experimental results for a full size SGM,[3,4,7,9] and show distinctive difference from staggered herringbone micromixer (SHM),[3,8,11] indicating that the proportional size reduction of the reported SGM will not change its nature of mixing enhancement.

To characterize the mixing process in more details, the concentrations at a fixed cross-section location but at various channel lengths along flow direction were collected from the simulation results and plotted as a function of channel length (i.e., concentration versus channel length profile) as shown in Fig. 3. The concentrations oscillate along the channel length regardless of their specific cross-section location. In comparing with the corresponding cross-section concentration images shown in the figure, which were used in literature as the standard way to characterize micromixing,[8,13] the concentration oscillation is believed to be caused by the helical flow described above and its related micromixing, and is associated with the helical flow of the fluids.

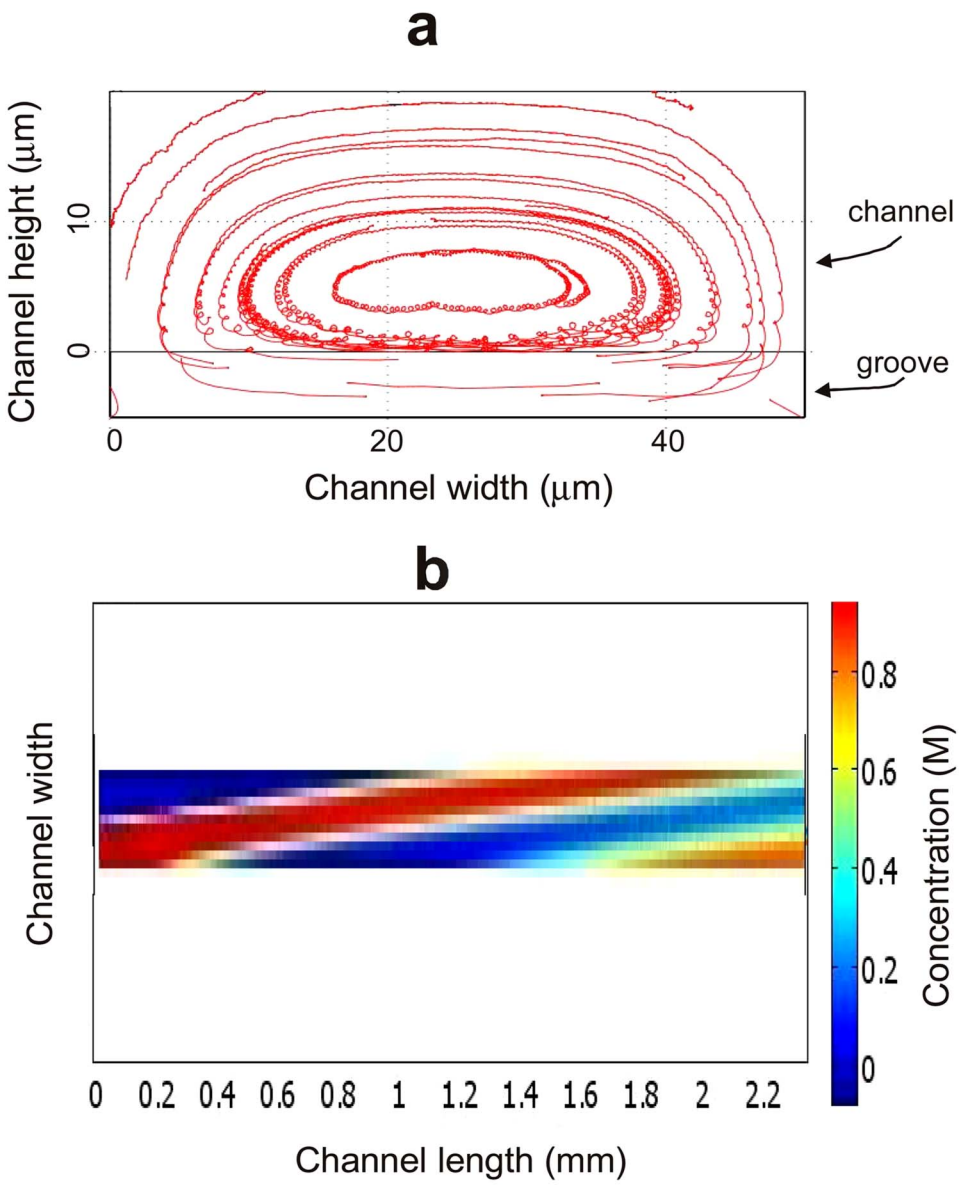

FIG. 2. Simulation results of the SGM with groove depth at 5 μm during the mixing process of a 1 M fluid with a 0 M fluid: (a) Cross-section streamlines of the fluids, showing the flow fell into the grooves and its caused helical flow within the channel; (b) concentration image of the fluids at their upper surface, showing the helical flow-caused rotation of the two mixing fluids within the channel.

As seen from the concentration at the top right location of the cross section (red letter *e*), it starts from 0 M at the channel inlet (dark blue color in the image and red line labeled as *e* in the concentration-length profile), increases, along the channel, to over 0.9 M when the fluid with 1 M concentration at inlet helically flows a channel length of 1.6 mm to the same cross-section location (red color in the image now). Afterwards, it goes down to 0.2 M when the lower-concentration fluid returns to the location (light blue in the image) at the channel length of 2.8 mm, and then increases to 0.7 M when the high-concentration fluid reenters the location at 4.1 mm (orange in the image). In other words, as the two mixing fluids flow helically and mix along the channel, the concentration at each cross-section location oscillates along the channel length accordingly. Each cycle of concentration oscillation directly corresponds to a helical-flow cycle and contains detailed

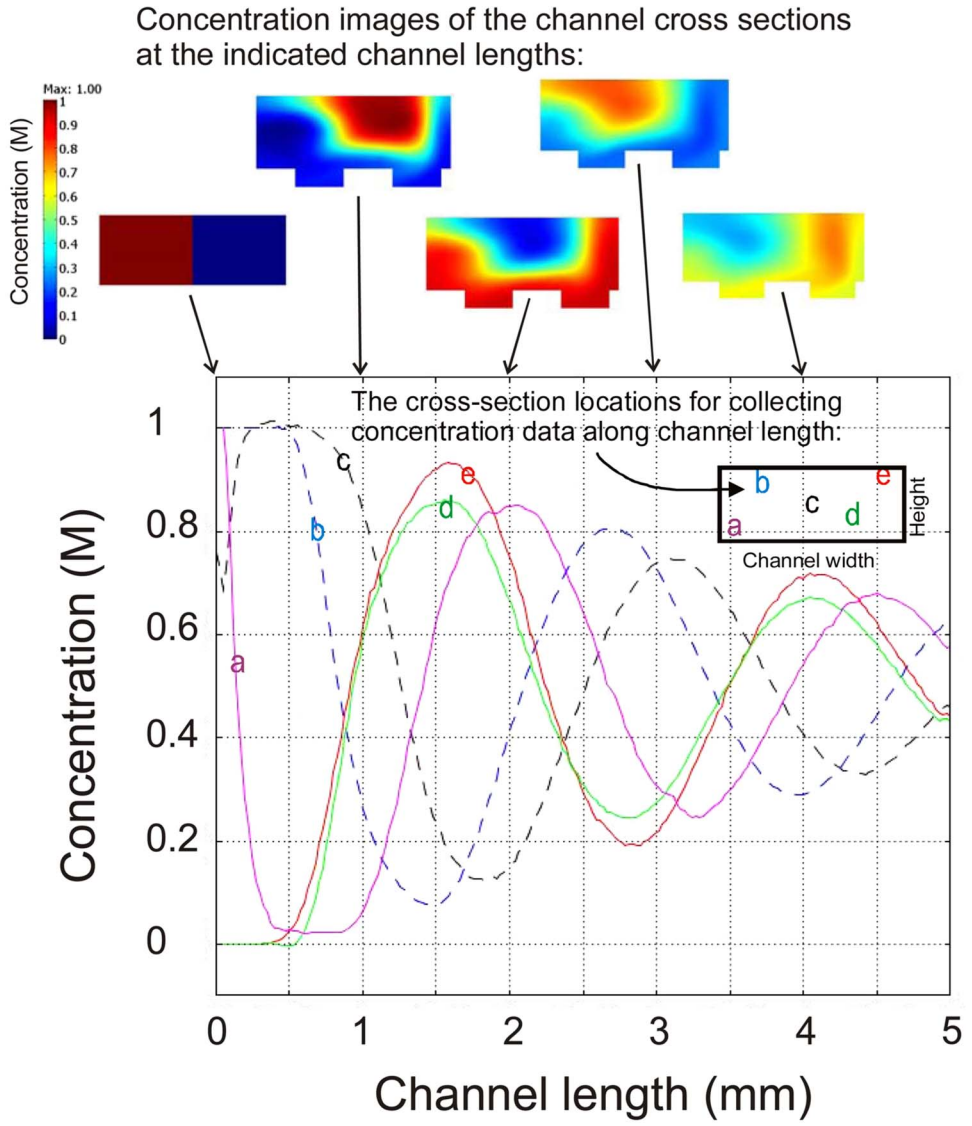

FIG. 3. Concentrations as a function of channel length for the SGM mixer with groove depth at 5 μm. The concentration data are collected along channel length in its flow direction at the fixed cross-section locations represented with purple at (6.25,6.5) (unit in μm); blue at (12.5,15); black at (25,10); red at (43.75,17.5), and green at (37.5,5) in the x–y coordinate system of the cross section with its left-down point set at (0,0) as indicated by the color-corresponding letters shown in the channel cross section. The concentration images of the channel cross sections are collected at the indicated channel lengths.

information about the associated molecular mixing within the cycle. This important concentration oscillation was not reported in literature before the method of using concentration–channel length profiles to characterize micromixing was first used in this work even though much research has been done to simulate and test this type of devices as seen in the listed literature. It has shown the known and, furthermore, revealed the unknown but in-depth information about the helical flow and its enhanced mixing.

From the concentration–channel length profiles, some new but critical parameters can be defined and used to characterize the micromixing. Apparently, the peak-to-peak or valley-to-valley pitches of the concentration oscillation correspond to the channel length required to complete a full helical-flow cycle (i.e., cycle pitch of the helical flow), and the peak-to-peak or valley-to-valley concentration changes are associated with the mixing efficiency. While the average pitch P_h

value can be directly obtained from the profile data, the mixing efficiency E_m can be expressed as the peak-to-peak or valley-to-valley concentration change during a helical cycle: $E_m=(C_i-C_{i+1})/C_iP_h$, where C is the concentration at the peak or valley and i is the order number of the peak or the valley. This E_m value captures the concentration change along channel length, which is the key for characterizing micromixing. While their values oscillate along channel length with the helical flow, the concentrations at various locations are all seen to converge toward 0.5 M which is the destination value for fully mixing the two fluids concentrated at 1 M and 0 M respectively. When the concentration in every location within the whole cross section reaches a value of $C=0.5\ \mathrm{M}\pm\varepsilon$ at a channel length L_m (mixing completion length), where ε is the targeted concentration uniformity according to a specific application, mixing can be considered completed at the position.

With the three aforementioned parameters, the helical flow, the mixing process, and the degree of mixing achieved within a SGM can be easily characterized. This concentration versus length profile-based method was further demonstrated in the analysis of the effects of groove geometry on the mixing performance of the SGM. Figure 4 shows the results for various SGMs which have identical device structure except their groove depth. By increasing the groove depth from 5 μm shown in Fig. 3 to 10, 20, and even 30 μm within the reported upper limit of the ratio of groove depth to channel height at 1.6 μm (Ref. 13) as shown in Fig. 4, the concentration oscillation becomes more frequent and substantial, and the concentration convergence becomes faster. The corresponding average pitch P_h value, mixing efficiency E_m, and mixing completion length L_m of each SGM were shown in Table I, where five cross-section locations within the channels, as shown in Figs. 3 and 4, were chosen from a middle-point type of mapping to represent the identified major zones for the calculation, so that a massive cross-section screening can be avoided. The data indicates that the helical pitch decreases and the mixing efficiency increase substantially with deepening the grooves, in agreement with the reported simulation and experimental results that deep grooves are in favor of mixing in SHM and SGM,[8,13] and extremely deep grooves in a SGM are very efficient in enhancing micromixing.[2] The mixing can be completed at a specific channel length of 5 mm when the groove depth is set at 20 μm and 3.6 mm at 30 μm. It shows that the three parameters are sufficient enough to quantitatively characterize the performance of each mixer and the effect of groove depth on mixing performance. With all the reported characterization methods, such as concentration images (also seen in Figs. 3 and 4), streaklines, and Pioncaré maps, on the other hand, a simulation can only tell a trend about the mixing caused by the groove depth.

Clearly, the described concentration-length profile based method is able to easily provide specific data to quantitatively, comprehensively, and directly characterize the micromixing occurring within a SGM. These capabilities are critical for achieving numerical simulation-based mixer design because, as demonstrated in the design of microelectronic and integrated photonic devices, a real device design requires specific performance data to find optimal device structure through numerical simulations. Unless the performance of a device is well defined and can be quantified in the process, a numerical simulation can only provide guidance, leaving optimal device structure to be found from massive experimental trials that are time consuming and costly. The summarized three parameters, including P_h, E_m, and particularly L_m, are obviously suitable for the use in designing the SGM as discussed earlier. They were also successfully used in analyzing and designing SHM and its combination with SGM in our effort to develop a high efficient mixer for dynamically labeling cells within microfluidic channels with a small channel dimension, and are believed to be applicable to all types of micromixers with grooved surface.

Concentration-based analysis, in principle, should be the most reliable method in studying molecular micromixing because every involved mixing component, such as bulk advection and molecular diffusion, will be eventually reflected in concentration change. It is obviously more comprehensive and representative than the particle tracking-based analysis that is used in characterizing chaotic micromixing,[5,6,9] but does not take the molecular diffusion that is important for a flow with low Reynolds number into account. Unfortunately, the current concentration-based analysis is still unable to provide in-depth and precise information about micromixing because of

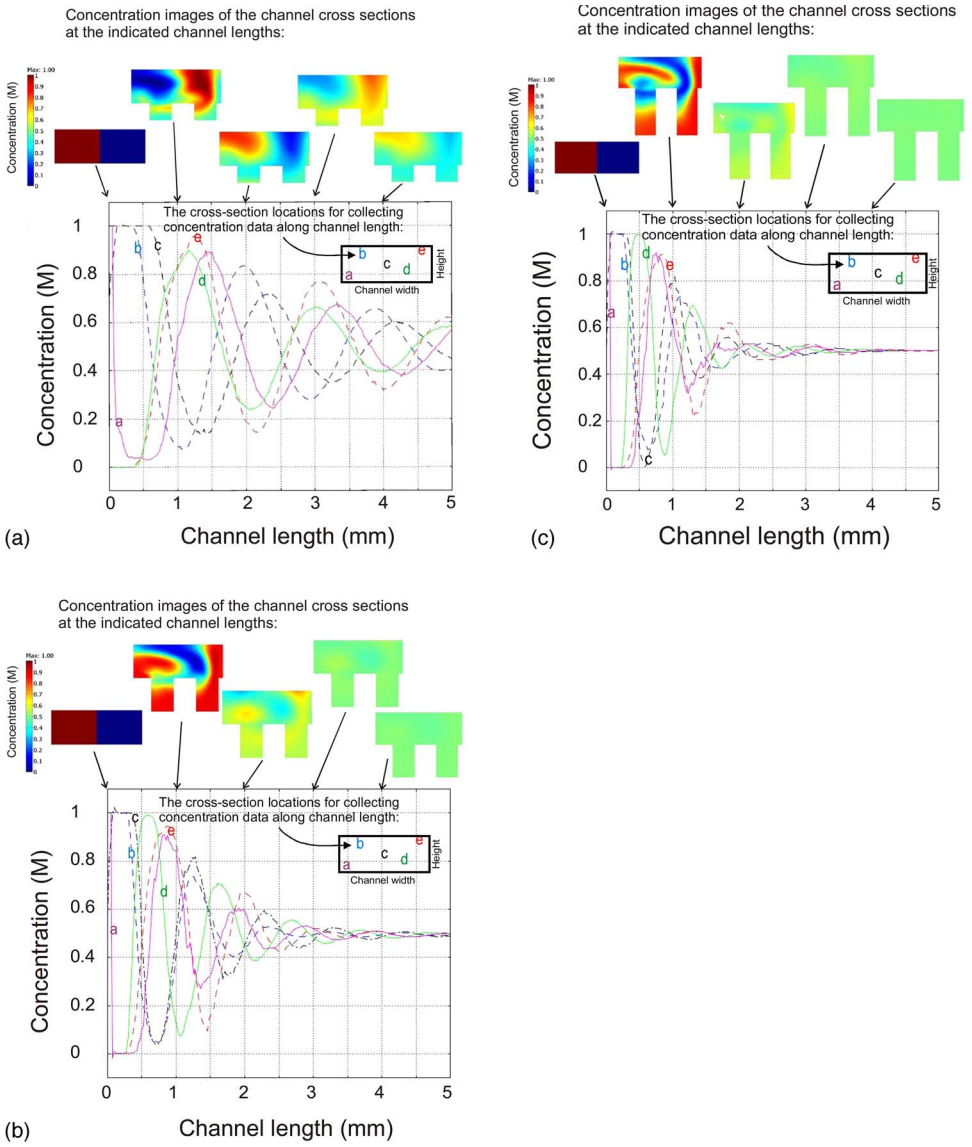

FIG. 4. Effects of groove depth on the concentration-channel profiles. Groove depth at (a) 10 μm; (b) 20 μm; and (c) 30 μm; the concentration data are collected at the cross-section locations described in Fig. 3 while the concentration images of the channel cross section are collected at the indicated channel lengths.

the lack of a quantitative method to characterize simulation results. By improving its characterization method from analyzing concentration images, as currently used in the literature, to processing specific concentration data, and very importantly, by correlating the data to channel length, as presented in this work, it becomes possible to reveal the detailed process within a micromixer. Note that micromixing occurs dynamically during the flow of the involved mixing fluids, and the concentration change along channel length is essential for understanding the process. The described concentration–channel length profiles have been shown to be able to catch the dynamic micromixing process of flowing fluids within a surface-grooved microfluidic channel, and should be applicable to the analysis of other type of micromixers in principle, as long as representative locations in the channel cross section are selected, according to the specific mixing mechanism, to follow the concentration change and sufficient critical performance parameters are properly defined. For instance, the method was demonstrated in characterizing the simulation of a classic *T*

TABLE I. Mixing performance of slant-grooved mixer.[a]

Groove depth (μm)	Cycle pitch P_h (mm)	Mixing efficiency E_m (mm^{-1}) [b]	Mixing completion length L_m (mm) at ε=0.01 M [c]
5	2.5	0.2	—[d]
10	1.9	0.3	—[d]
20	1.0	0.7	5.0
30	0.7	1.2	3.6

[a]Calculated from the five cross-section locations as shown in Figs. 3 and 4.
[b]Averaged from first measurable peak-to-peak.
[c]Concentrations at the five cross-section locations are converged to 0.5 M $\pm \varepsilon$.
[d]The concentration does not converge to 0.5 $\pm$ 0.01 M within the simulated 5-mm channel length and cannot be calculated from the simulation results.

mixer, in which mixing is purely controlled by the diffusion between the two involved fluids through their interface. As shown in Fig. 5, while the concentration at the interface of the two fluids instantly reaches their neutral zone at 0.5 M, the concentration at its adjacent locations gradually drifts or converges toward the zone because of the involved molecular diffusion. Such a concentration convergence is rapid at its initial stage, especially, at the cross-section location

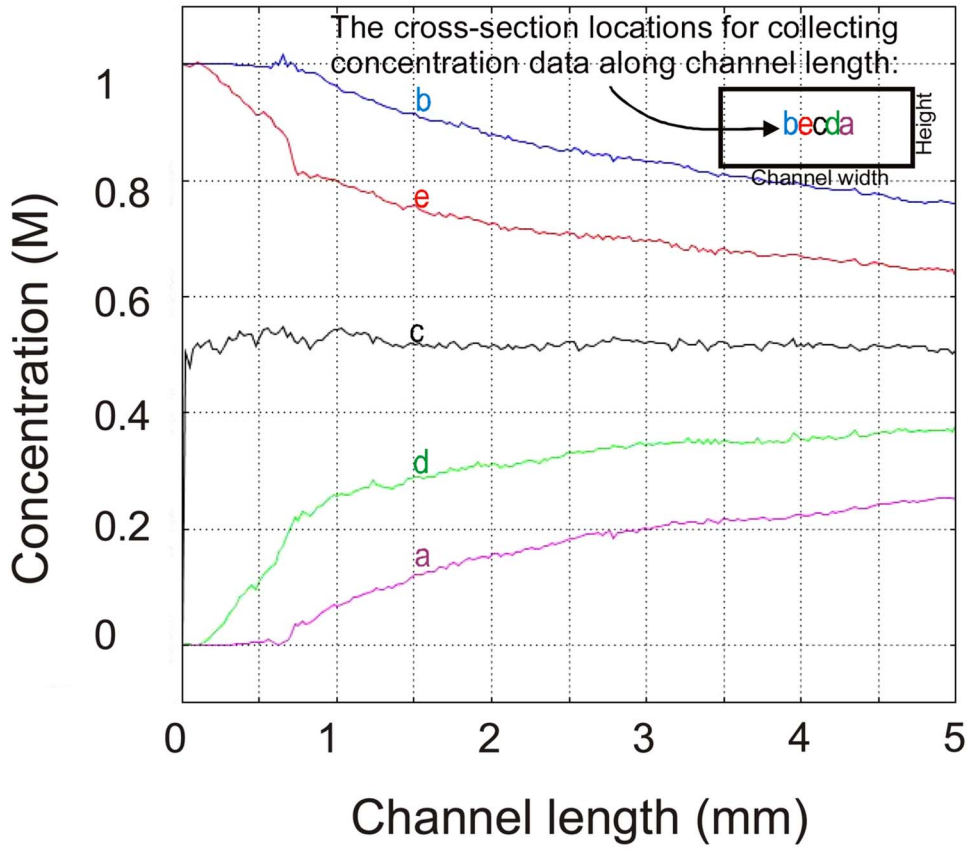

FIG. 5. Concentrations as a function of channel length for a *T*-mixer with a channel dimension of 20 μm (height) $\times$50 μm (width). Concentration data are collected along channel in its flow direction at the fixed cross-section locations (in μm) represented with blue at (19,10); red at (22,10); black (25,10); green at (28,10), and green at (31,10) in the x–y coordinate system of the cross section with its left-down point set at (0,0) as indicated by the color-corresponding letters shown in the channel cross section. The device structure is the same as that shown in Fig. 1 except there are no grooves on the channel floor.

closer to the interface, and gradually slows down with the fluids flowing along the channel, demonstrating the well-known effect of concentration gradient on diffusion speed. Note that other methods, such as concentration images, are unable to characterize the concentration gradient-related process. In this application, the concentration-length slope $\delta C/\delta L$ can be used to characterize the mixing efficiency E_m at each cross-section location and the channel length required for the concentration at channel edges to reach $C=0.5\ \mathrm{M}\pm\varepsilon$ is the mixing completion length L_m.

IV. CONCLUSION

In conclusion, the micromixing within floor-grooved microfluidic channels was numerically simulated using commercial software and was characterized using the obtained concentrations as a function of channel lengths. Concentration at various locations of the channel cross section was found to periodically oscillate along the channel length and gradually converge to the neutral concentration of the two mixing fluids. This concentration oscillation corresponds to the groove-caused helical flow and can provide quantitative, direct, and comprehensive information about the flow and its associated mixing involved with molecular diffusion. Therefore, three performance parameters, including helical flow cycling length P_h, mixing efficiency E_m, and mixing completion length L_m were easily defined and calculated, and were used to study the effects of groove geometry on the mixing. This concentration versus channel length profile-based method was also demonstrated in characterizing the mixing process in a classic T micromixer and is suggested applicable to other types of micromixers. It focuses on specific concentration data, which is the most reliable information for analyzing micromixing, and correlates the data to channel length to capture the dynamic process that occurs during the flow of the involved mixing fluids. The method has two clear advantages over other reported characterization methods: (i) It can directly reveal the details of a mixing process and is useful for mechanism and process study; and (ii) it can provide specific performance data to quantitatively, directly, and comprehensively evaluate a mixer. The latter one is very important for optimizing device structure through numerical simulation in our view because the optimization, which can minimize experimental trials, needs well-defined performance data to work on. Numerical simulation is playing a vital role in developing microelectronic and integrated photonic devices, and should greatly benefit the development of microfluidic devices when it is effectively used in the field.

ACKNOWLEDGMENTS

This work is supported, in part, by a Strategic Grant by the Natural Sciences and Engineering Research Council of Canada (NSERC).

[1] V. Hessel, H. Lowe, and F. Schonfeld, Chem. Eng. Sci. **60**, 2479 (2005).
[2] T. J. Johnson, D. Ross, and L. E. Locascio, Anal. Chem. **74**, 45 (2002).
[3] A. D. Stroock, S. K. Dertinger, A. Ajdar, I. Mezic, H. A. Stone, and G. M. Whitesides, Science **295**, 647 (2002).
[4] H. Wang, P. Iovenitti, E. Harvey, and S. Masood, J. Micromech. Microeng. **13**, 801 (2003).
[5] J. Aubin, D. F. Fletcher, J. Bertrand, and C. Xuereb, Chem. Eng. Technol. **26**, 1262 (2003).
[6] T. G. Kang and T. H. Kwon, J. Micromech. Microeng. **14**, 891 (2004).
[7] A. D. Stroock, S. K. Dertinger, G. M. Whitesides, and A. Ajdari, Anal. Chem. **74**, 5306 (2002).
[8] J. T. Yang, K. J. Huang, and Y. C. Lin, Lab Chip **5**, 1140 (2005).
[9] J. T. Yang, K. J. Huang, I. C. Hu, and P. C. Lyu, J. Micromech. Microeng. **17**, 2084 (2007).
[10] J. Aubin, D. F. Fletcher, and C. Xuereb, Chem. Eng. Sci. **60**, 2503 (2005).
[11] M. A. Ansari and K. Y. Kim, Chem. Eng. Sci. **62**, 6687 (2007).
[12] D. G. Hassell and W. B. Zimmerman, Chem. Eng. Sci. **61**, 2977 (2006).
[13] T. J. Johnson and L. E. Locascio, Lab Chip **2**, 135 (2002).
[14] E. Villermaux, A. D. Strook, and H. A. Stone, Phys. Rev. E **77**, 015301 (2008).